

TESS DISCOVERY OF A TRANSITING SUPER-EARTH IN THE π MENSAE SYSTEM

CHELSEA X. HUANG^{1,2}, JENNIFER BURT^{1,2}, ANDREW VANDERBURG^{3,4}, MAXIMILIAN N. GÜNTHER^{1,2}, AVI SHPORER¹, JASON A. DITTMANN^{5,6}, JOSHUA N. WINN⁷, ROB WITTENMYER⁸, LIZHOU SHA¹, STEPHEN R. KANE⁹, GEORGE R. RICKER¹, ROLAND K. VANDERSPEK¹, DAVID W. LATHAM¹⁰, SARA SEAGER^{1,6}, JON M. JENKINS¹¹, DOUGLAS A. CALDWELL^{11,12}, KAREN A. COLLINS¹⁰, NATALIA GUERRERO¹, JEFFREY C. SMITH¹², SAMUEL N. QUINN¹¹, STÉPHANE UDRY¹³, FRANCESCO PEPE¹³, FRANÇOIS BOUCHY¹³, DAMIEN SÉGRANSAN¹³, CHRISTOPHE LOVIS¹³, DAVID EHRENREICH¹³, MAXIME MARMIER¹³, MICHEL MAYOR¹³, BILL WOHLER^{11,12}, KARI HAWORTH¹, EDWARD H. MORGAN¹, MICHAEL FAUSNAUGH¹, DAVID R. CIARDI¹⁴, JESSIE CHRISTIANSEN¹⁴, DAVID CHARBONNEAU¹⁰, DIANA DRAGOMIR^{1,15}, DRAKE DEMING¹⁶, ANA GLIDDEN^{1,6}, ALAN M. LEVINE¹, P.R. McCULLOUGH¹⁷, LIANG YU¹, NORIO NARITA^{18,19,20,21,22}, TAM NGUYEN¹, TIM MORTON⁷, JOSHUA PEPPER²³, ANDRÁS PÁL^{1,24,25}, JOSEPH E. RODRIGUEZ¹⁰, AND THE TESS TEAM

Draft version November 9, 2018

ABSTRACT

We report the detection of a transiting planet around π Men (HD 39091), using data from the *Transiting Exoplanet Survey Satellite* (TESS). The solar-type host star is unusually bright ($V = 5.7$) and was already known to host a Jovian planet on a highly eccentric, 5.7-year orbit. The newly discovered planet has a size of $2.04 \pm 0.05 R_{\oplus}$ and an orbital period of 6.27 days. Radial-velocity data from the HARPS and AAT/UCLES archives also displays a 6.27-day periodicity, confirming the existence of the planet and leading to a mass determination of $4.82 \pm 0.85 M_{\oplus}$. The star's proximity and brightness will facilitate further investigations, such as atmospheric spectroscopy, asteroseismology, the Rossiter–McLaughlin effect, astrometry, and direct imaging.

Subject headings: planetary systems, planets and satellites: detection, stars: individual (HD 39091, TIC 261136679)

¹ Department of Physics, and Kavli Institute for Astrophysics and Space Research, Massachusetts Institute of Technology, Cambridge, MA 02139, USA

² Juan Carlos Torres Fellow

³ Department of Astronomy, The University of Texas at Austin, Austin, TX 78712, USA

⁴ NASA Sagan Fellow

⁵ 51 Pegasi b Postdoctoral Fellow

⁶ Earth and Planetary Sciences, MIT, 77 Massachusetts Avenue, Cambridge, MA 02139, USA

⁷ Department of Astrophysical Sciences, Princeton University, 4 Ivy Lane, Princeton, NJ 08544, USA

⁸ University of Southern Queensland, West St, Darling Heights QLD 4350, Australia

⁹ Department of Earth Sciences, University of California, Riverside, CA 92521, USA

¹⁰ Harvard–Smithsonian Center for Astrophysics, Harvard University, Cambridge, MA 02138, USA

¹¹ NASA Ames Research Center, Moffett Field, CA, 94035

¹² SETI Institute, Mountain View, CA 94043, USA

¹³ Observatoire de l'Université de Genève, 51 chemin des Maillettes, 1290 Versoix, Switzerland

¹⁴ NASA Exoplanet Science Institute, Caltech/IPAC-NExScI 1200 East California Boulevard Pasadena, CA 91125

¹⁵ NASA Hubble Fellow

¹⁶ Department of Astronomy, University of Maryland at College Park, College Park MD, 20742

¹⁷ Department of Physics and Astronomy, Johns Hopkins University, 3400 North Charles Street, Baltimore, MD 21218, USA

¹⁸ Department of Astronomy, The University of Tokyo, 7-3-1 Hongo, Bunkyo-ku, Tokyo 113-0033, Japan

¹⁹ Astrobiology Center, National Astronomical Observatory of Japan, NINS, 2-21-1 Osawa, Mitaka, Tokyo 181-8588, Japan

²⁰ JST, PRESTO, 7-3-1 Hongo, Bunkyo-ku, Tokyo 113-0033, Japan

²¹ Instituto de Astrofísica de Canarias (IAC), 38205 La Laguna, Tenerife, Spain

²² National Astronomical Observatory of Japan, NINS, 2-21-1 Osawa, Mitaka, Tokyo 181-8588, Japan

²³ Department of Physics, Lehigh University, 16 Memorial Drive East, Bethlehem, PA 18015, USA

²⁴ Department of Astronomy, Loránd Eötvös University, Pázmány P. stny. 1/A, Budapest H-1117, Hungary

²⁵ Konkoly Observatory, Research Centre for Astronomy and Earth Sciences, Hungarian Academy of Sciences, Konkoly Thege Miklós út 15-17, H-1121 Budapest, Hungary

1. INTRODUCTION

The mission of the *Transiting Exoplanet Survey Satellite* (*TESS*, Ricker et al. 2015) is to search for transiting planets as small as Earth around the nearest and brightest stars. Four 10 cm optical telescopes are used to repeatedly image wide fields and monitor the brightness of suitable stars. The data are then searched for periodic dips that could be caused by transiting planets. The spacecraft was launched on April 18, 2018 and began the sky survey on July 25. Here, we report on the discovery of a small transiting planet around a bright star π Men.

π Men (also known as HD 39091) is a naked-eye G0V star at a distance of 18.27 ± 0.02 pc (Gaia Collaboration et al. 2018) with a mass of $1.1 M_{\odot}$ and a radius of $1.1 R_{\odot}$. Doppler monitoring by Jones et al. (2002) and Wittenmyer et al. (2012) revealed a planet (π Men b) with a mass about 10 times that of Jupiter, an orbital period of 5.7 years, and an orbital eccentricity of 0.6. With a visual apparent magnitude of 5.67, the star is a prime target for the *TESS* survey. It is one of several hundred thousand pre-selected stars for which data will be available with 2-minute time sampling, as opposed to the 30-minute sampling of the full image data set.

This *Letter* is organized as follows. Section 2 presents the *TESS* photometric data that led to the detection of the new planet π Men c, as well as the archival radial velocity data that confirm the planet’s existence. Section 3 describes our methods for determining the system parameters, including the mass and radius of the star and planet. Section 4 discusses some possible follow-up observations that will be facilitated by the star’s brightness and proximity to Earth.

2. OBSERVATIONS AND DATA REDUCTION

2.1. *TESS photometry*

The *TESS* survey divides the sky into 26 partially overlapping sectors, each of which is observed for approximately one month during the two-year primary mission. π Men is located near the southern ecliptic pole in a region where 6 sectors overlap, implying that it is scheduled to be observed for a total of 6 months. This paper is based on data from Sector 1 (2018 July 25 – August 22), during which π Men was observed with CCD 2 of Camera 4.

The data were processed with two independently written codes: the MIT Quick Look Pipeline (partially based on `fitsh`, ?), which analyzes the full images that are obtained with 30-minute time sampling; and the Science Processing Operations Center pipeline, a descendant of the *Kepler* mission pipeline based at the NASA Ames Research Center (Jenkins et al. 2010), which analyzes the 2-minute data that are obtained for pre-selected target stars. For π Men, both pipelines detected a signal with a period of 6.27 days, an amplitude of about 300 ppm, a duration of 3 hours, and a flat-bottomed shape consistent with the light curve of a planetary transit.

Previous surveys taught us that transit-like signals sometimes turn out to be eclipsing binaries that are either grazing, or blended with a bright star, causing the amplitude of the signal to be deceptively small and resemble that of a planet (e.g. Cameron 2012). In this case, the signal survived all the usual tests for such “false positives.” There is no discernible secondary eclipse, no

detectable alternation in the depth of the transits, and no detectable motion of the stellar image on the detector during the fading events.²⁶

After identifying the transits, we tried improving on the light curve by experimenting with different choices for the photometric aperture, including circles as well as irregular pixel boundaries that enclose the blooming stellar image. Best results were obtained for the aperture shown in Figure 1. Also shown are images of the field from optical sky surveys conducted 30–40 years ago, long enough for the star to have moved about an arcminute relative to the background stars. This allows us a clear view along the line of sight to the current position of π Men, which is reassuringly blank: another indication that the transit signal is genuine and not an unresolved eclipsing binary. The other stars within the photometric aperture are too faint to cause the 300 ppm fading events.

The top panel of Figure 2 shows the result of simple aperture photometry. Most of the observed variation is instrumental. There may also be a contribution from stellar variability, which is expected to occur on the 18-day timescale of the rotation period (Zurlo et al. 2018). To remove these variations and permit a sensitive search for transits, we fitted a basis spline with knots spaced by 0.3 days, after excluding both 3σ outliers and the data obtained during and immediately surrounding transits. We then divided the light curve by the best-fitting spline.

The middle panel of Figure 2 shows the result. The scatter is 142 ppm per 2-minute sample, and 30 ppm when averaged into 6-hour bins, comparable to the highest-quality *Kepler* light curves. The gap in the middle of the time series occurred when observations were halted for data downlink. The other gap occurred during a period when the spacecraft pointing jitter was higher than normal. We also excluded the data from the 30–60 minute intervals surrounding “momentum dumps,” when thrusters are fired to reorient the spacecraft and allow the reaction wheels to spin down. The times of the momentum dumps are marked in Figure 2. There were 10 such events during Sector 1 observations, occurring every 2 and half days.

2.2. *Radial-velocity data*

π Men has been monitored for 20 years as part of the Anglo-Australian Planet Search, which uses the 3.9m Anglo-Australian Telescope (AAT) and the University College London Echelle Spectrograph (UCLES; Diego et al. 1990). The long-period giant planet π Men b was discovered in this survey (Jones et al. 2002; Butler et al. 2006). A total of 77 radial velocities are available, obtained between 1998 and 2015, with a mean internal uncertainty of 2.13 m s^{-1} .

The star was also monitored with the High-Accuracy Radial-velocity Planet Searcher HARPS (Mayor et al. 2003) on the ESO 3.6m telescope at La Silla Observatory in Chile. A hardware upgrade in June 2015 led to an offset in the velocity scale (Lo Curto et al. 2015). For this reason, our model allows for different constants to be added to the pre-upgrade and post-upgrade data. A total

²⁶ The last test in the list, the centroid test, was complicated by the fact that the star is bright enough to cause blooming in the *TESS* CCD images. The associated systematic effects were removed using the method of Günther et al. (2017).

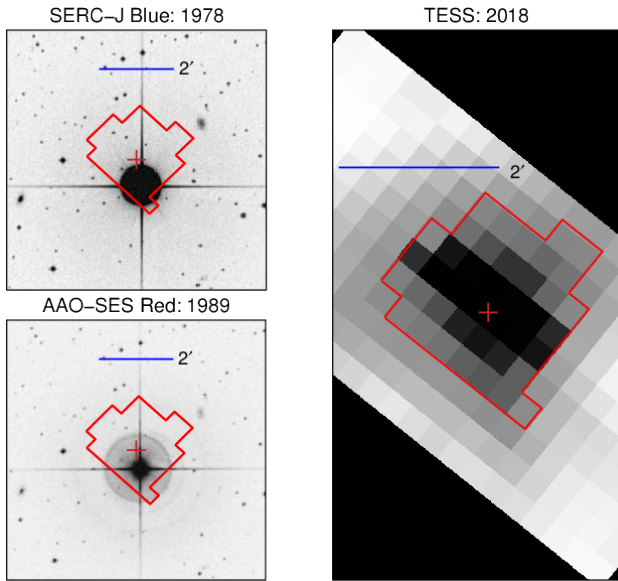


FIG. 1.— Images of the field surrounding π Men. *Top left.*—From the Science and Engineering Research Council J survey, obtained with a blue-sensitive photographic emulsion in 1978. The red cross is the current position of π Men. Red lines mark the boundary of the *TESS* photometric aperture. *Bottom left.*—From the AAO Second Epoch Survey, obtained with a red-sensitive photographic emulsion in 1989. *Right.*—Summed *TESS* image. North is up and East is to the left in all the images.

of 145 radial velocities are available, obtained between December 2003 and March 2016 with irregular sampling. The mean internal uncertainty of the 128 pre-upgrade velocities is 0.78 m s^{-1} , while that of the 17 post-upgrade velocities is 0.38 m s^{-1} .

The top panel of Figure 3 shows the radial-velocity data. It is easy to see the 400 m s^{-1} variations from the giant planet. To search for evidence of the new planet, we subtracted the best-fitting single-planet model from the data and computed the Lomb–Scargle periodogram of the more precise HARPS data, shown in the middle panel. The highest peak is far above the 0.1% false alarm threshold and is located at the transit period of 6.27 days. The next highest peaks, bracketing a period of 1 day, are aliases of this signal. The phase of the 6.27-day signal is also consistent with the measured transit times.

We consider this to be a decisive confirmation of the existence of π Men c. Still, as another precaution against false positives, we checked the HARPS spectra for any indication of a second star, or spectral-line distortions associated with the 6.27-day signal. We re-analyzed the HARPS cross-correlation functions with the BLENDFITTER routine (Günther et al. 2018) and found no sign of any correlated bisector variations.

3. DETERMINATION OF SYSTEM PARAMETERS

We performed a joint analysis of the two-planet system using the *TESS* transit light curve and the 222 radial velocities from the AAT and HARPS surveys. The orbit of planet c was assumed to be circular in the fit.²⁷ As noted previously, we assigned a different additive con-

²⁷ We also tried allowing planet c to have an eccentric orbit, which resulted in an upper limit of $e_c < 0.3 (1\sigma)$. **All of the other orbital parameters remained consistent with the results of the $e_c \equiv 0$ model, although naturally, some parameters were subject to slightly larger uncertainties.**

stant to each of the 3 radial-velocity data sets. We also allowed for 3 independent values of the “jitter”, a term that is added in quadrature to the internally-estimated measurement uncertainty to account for systematic effects.

We assumed the star to follow a quadratic limb-darkening law and used the formulas of Mandel & Agol (2002) as implemented by Kreidberg (2015). We fixed the limb-darkening coefficients at $u_1 = 0.28$ and $u_2 = 0.27$, based on the tabulation of Claret (2017). The photometric model was computed with 0.4 min sampling and then averaged to 2 min before comparing with the data.

We also fitted for the mass and radius of the star, which were constrained by measurements of the spectroscopic parameters (Ghezzi et al. 2010) as well as the stellar mean density ρ_* implicit in the combination of P , a/R_* , and i (Seager & Mallén-Ornelas 2003; Winn 2010). For a given choice of mass, age, and metallicity, we relied on the Dartmouth stellar-evolutionary models (Dotter et al. 2008) to determine the corresponding radius R_* , effective temperature T_{eff} , and *Gaia* absolute magnitude. The likelihood function enforced agreement with the measurements of T_{eff} , ρ_* , $\log g$, and parallax (based on the absolute and apparent *Gaia* magnitudes).

To determine the credible intervals for all the parameters, we used the Markov Chain Monte Carlo (MCMC) method as implemented in *emcee* by Foreman-Mackey et al. (2013a). Detrending was performed simultaneously with the transit fitting: at each step in the Markov Chain, the transit model (*batman*, Kreidberg (2015)) was subtracted from the data and the residual light curve was detrended using a basis spline with knots spaced by 0.5 days. To avoid trying to model the discontinuities in the data related to momentum dumps, we only fitted the segment of the light curve in between momentum dumps. The results are given in Table 1 and Table 2, and the best-fitting model is plotted in Figures 2 and 3. As a consistency check, we also fitted each of the 5 transits independently. Figure 4 shows the results, which are all consistent to within the estimated uncertainties.

4. DISCUSSION

Among the known stars with transiting planets, π Men is the second brightest in the visual band, as illustrated in the top panel of Figure 5. *TESS* has begun to fulfill its promise to enlarge the collection of small, transiting planets orbiting bright stars. Such stars enable precise measurements of that planet’s mass and radius. The bottom panel of Figure 5 shows the measured masses and radii of the known planets smaller than Neptune, overlaid with theoretical mass/radius relationships for different compositions. π Men c falls above the “pure rock” curve on the diagram, and near curves for planets composed of either pure water or rocky interiors surrounded by a lightweight 1% H/He envelope. π Men c must not have a purely rocky composition, but instead may have a rocky core surrounded by layers of volatiles, such as hydrogen/helium (see Owen & Wu (2017)), or water/methane (Vanderburg et al. 2017).

With a near-infrared magnitude of $K = 4.24$, π Men is also one of the brightest stars available for planetary atmospheric characterization with the *James Webb Space Telescope (JWST)*. π Men c is one of the top 10 most favorable systems in the ranking scheme of Kempton

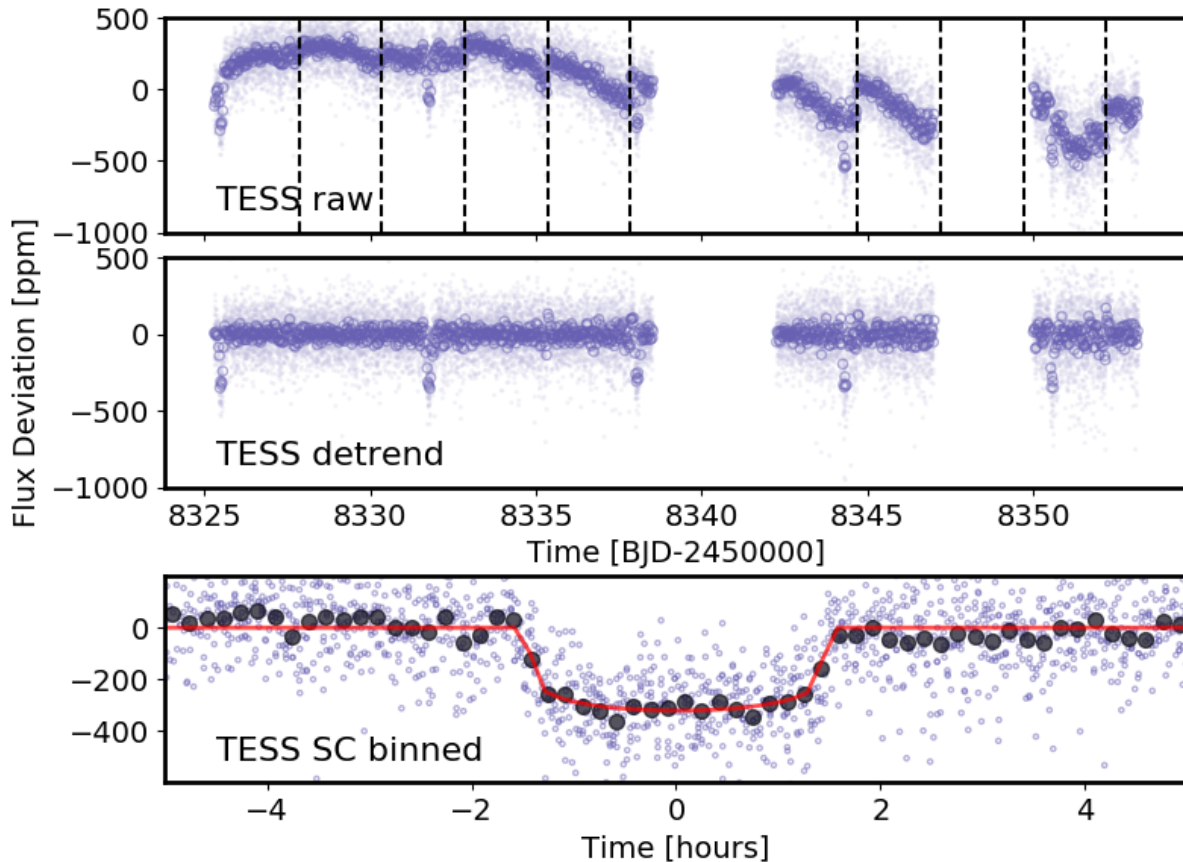


FIG. 2.— Raw (*top*) and corrected (*middle*) *TESS* light curves. The lighter points are based on the short cadence (SC) data with 2-minute sampling. The darker points are 30-minute averages. The dashed lines indicate the times of momentum dumps. The interruptions are from the data downlink and the pointing anomaly. The bottom panel shows the phase-folded light curve, along with the best-fitting model. The black dots represent 5-minute averages.

et al. (2018), although this ranking scheme does not take into account the practical difficulties in achieving photon-limited observations of such a bright star. Transit spectroscopy would be difficult if the planet has an Earth-like atmospheric scale height of order 10 km, in which case the atmospheric signals would be on the order of only 1 ppm. On the other hand, given the intense stellar irradiation, there may be larger signals from an escaping atmosphere (see, e.g., Ehrenreich et al. 2015; Spake et al. 2018). Spectroscopy of occultations (secondary eclipses) is also promising. The occultation depth is predicted to be 60 ppm in the Rayleigh-Jeans limit, assuming the entire surface radiates as a blackbody at the equilibrium temperature of 1200 K.

Another interesting possibility is to measure the stellar obliquity by observing the Rossiter–McLaughlin (RM) effect. Stars with close-in giant planets show a surprising diversity of orientations (Winn & Fabrycky 2015; Triaud 2017). However, we know relatively little about the obliquities of stars with smaller planets, because the relevant signals are smaller and harder to detect. In the case of π Men c, the amplitude of the RM effect is on the order of 1 m s^{-1} , the product of the transit depth (300 ppm) and the sky-projected rotation velocity (3.1 km s^{-1} ; Valenti & Fischer 2005a).

The π Men system consists of a giant planet on a long-period, highly eccentric orbit, along with a planet with an orbit and mass that are both smaller by two orders of magnitude. Recent follow-up studies of *Kepler* systems have suggested that they may be intrinsically common (Bryan et al. 2018; Zhu & Wu 2018). Thus, we might find many similar cases with *TESS*, providing clues about the formation of close-orbiting planets, whether by disk migration, Lidov–Kozai oscillations, or other mechanisms.

Astrometric observations with the *Gaia* spacecraft might ultimately reveal the full three-dimensional geometry of the system. Ranalli et al. (2018) predicted that the astrometric signal of π Men b will be detectable with a signal-to-noise ratio higher than 10 by the end of the mission. Indeed, the fit to the existing *Gaia* data exhibits an excess scatter of $295 \mu''$ (37σ), perhaps a hint of planet-induced motion. Direct imaging might also be fruitful some day, although Zurlò et al. (2018) have already ruled out any companions with orbital separation 10–20 AU and an infrared contrast exceeding 10^{-6} , corresponding roughly to 30 Jupiter masses.

While some of these observations may be far off, we will not have to wait long for another opportunity to learn more about π Men. As mentioned earlier, *TESS* is scheduled to collect 5 additional months of data. This

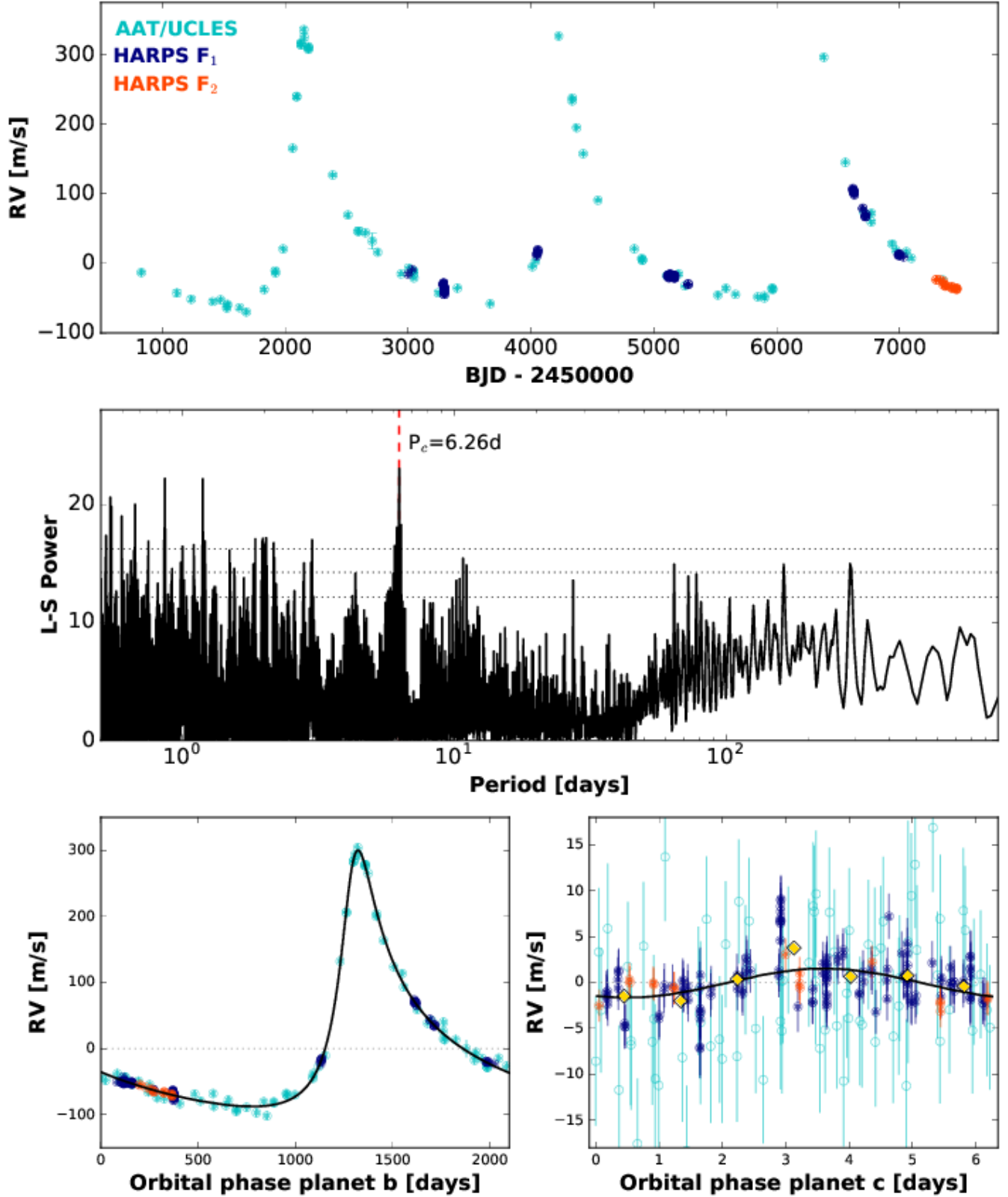


FIG. 3.— *Top*.—Relative radial velocity of π Men as measured with UCLES and HARPS (both pre- and post-upgrade). The zero points of each of the 3 datasets have been adjusted to coincide. *Middle*.—Lomb–Scargle periodogram of the HARPS data, after subtracting the single-planet model that best fits the entire data set. The dotted lines are the power levels corresponding to false alarm probabilities of 10%, 1%, and 0.1%. *Bottom left*.—Radial velocity as a function of the orbital phase of planet b, after subtracting the best-fitting model for the variation due to planet c. *Bottom right*.—Similar, but for planet c. The orange point is binned in phase space.

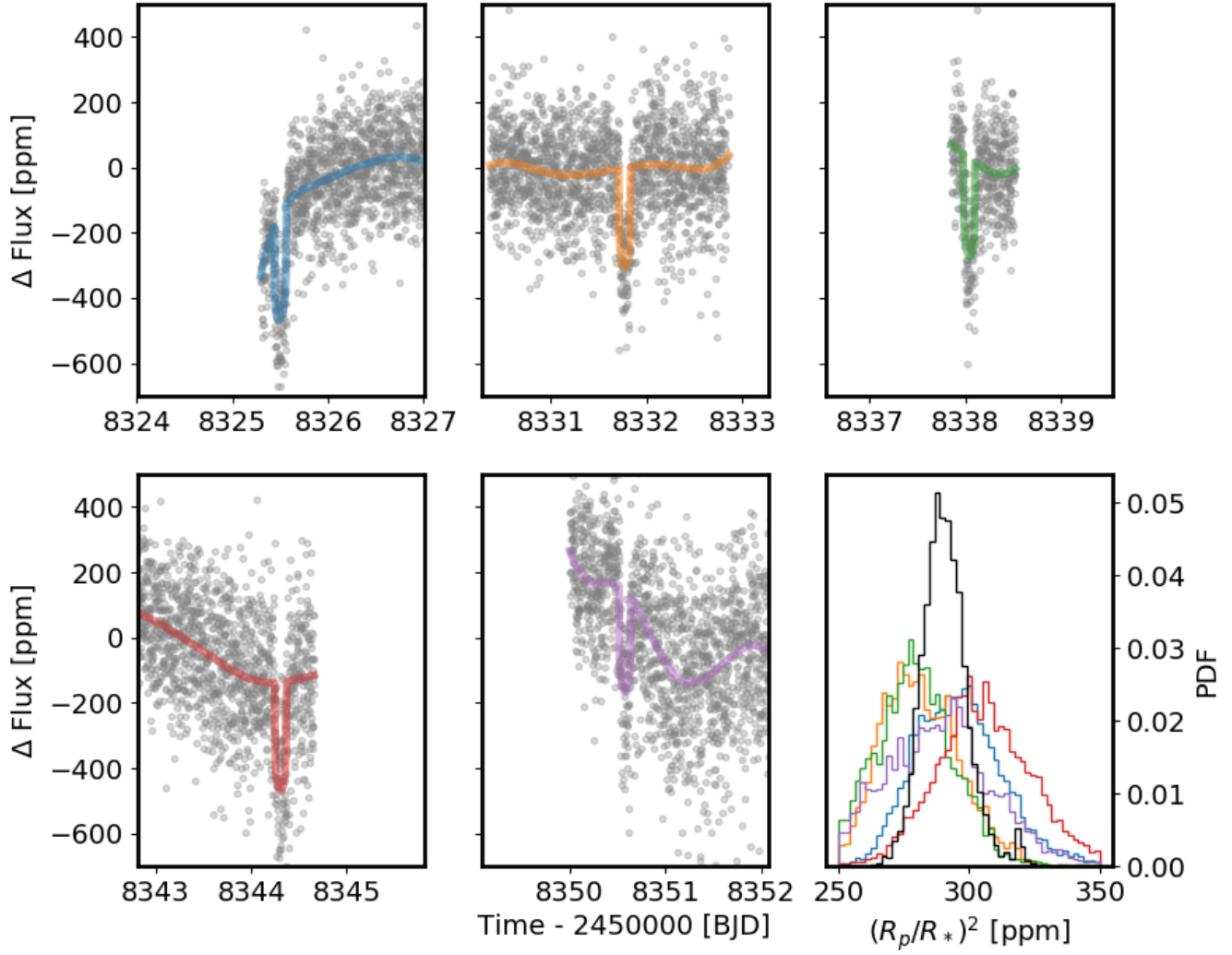


FIG. 4.— Plotted are the *TESS* data that surround each of the five observed transits and were obtained in between momentum dumps. Each panel shows 3 days of data and spans the same range of flux deviations. In the bottom right panel, the colored histograms are the 5 posterior distributions for $(R_p/R_*)^2$, obtained from independent fits to the 5 transit datasets. The black histogram is the posterior based on the fit to all the data.

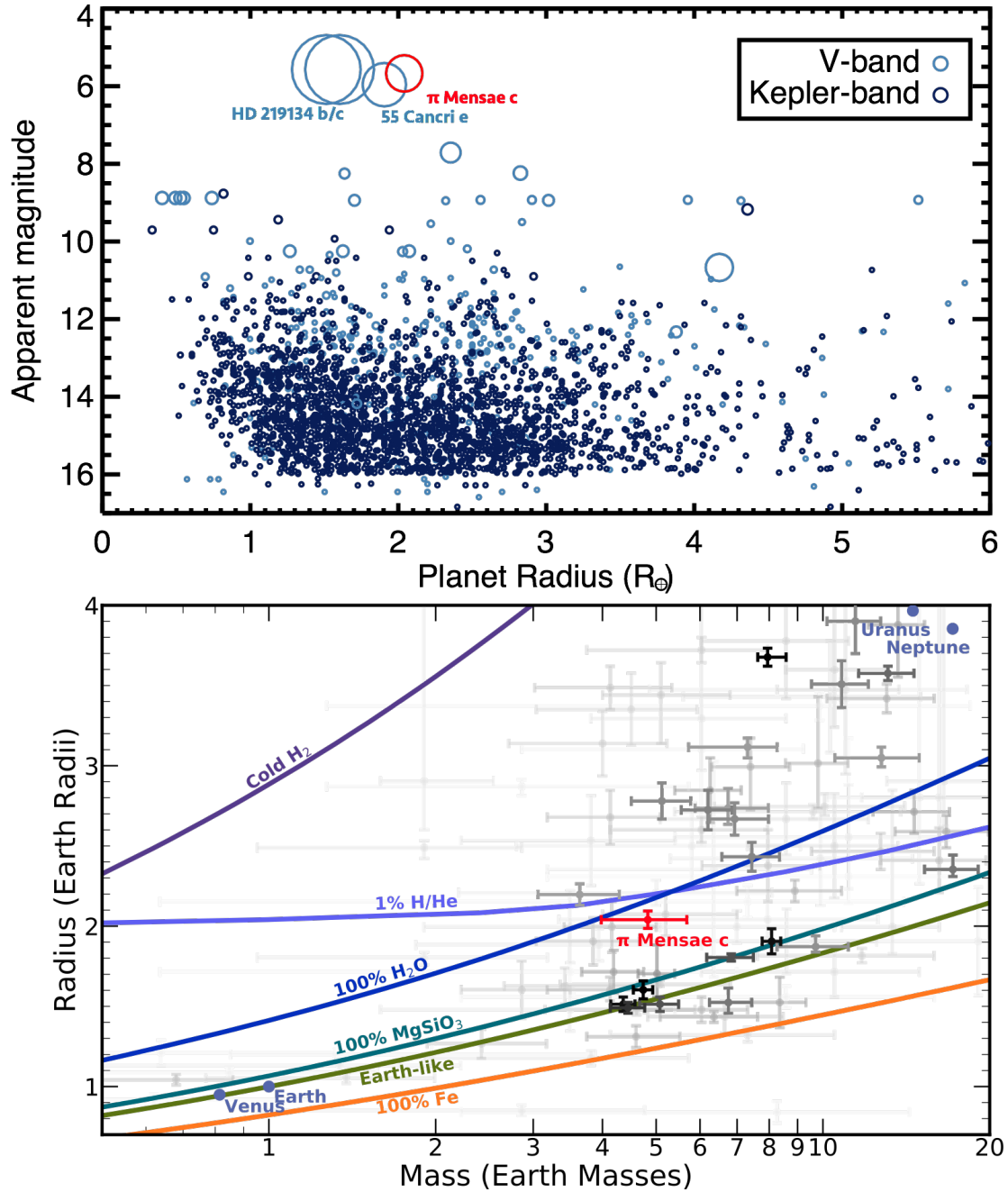


FIG. 5.— π Men c in the context of other known exoplanets. *Top.*—Apparent magnitude and planet radius for all the known transiting planets. The V magnitude is plotted when available, and otherwise the *Kepler* magnitude is plotted. The symbol size is proportional to the angular diameter of the star. *Bottom.*—Mass-radius diagram for small exoplanets. Darker points represent more precise measurements. Based on data from the NASA Exoplanet Archive, accessed on 13 September 2018.^a Model curves are: H_2 (Seager et al. 2007); 100% H_2O , 100% $MgSiO_3$, 100% Fe , Earth like (Zeng et al. 2016); and 1 % H/He (Lopez et al. 2012).

^a<https://exoplanetarchive.ipac.caltech.edu/cgi-bin/TblView/nph-tblView?app=ExoTbls&config=planets>

will allow us to refine our knowledge of planet c, search for additional transiting planets, and try to detect asteroseismic oscillations. The π Men system has already been generous to the exoplanet community, and with a little luck, the gifts will keep arriving.

TABLE 1
SYSTEM PARAMETERS FOR π MEN

Stellar Parameters	Value	Source
Catalog Information		
R.A. (h:m:s)	05:37:09.89	<i>Gaia</i> DR2
Dec. (d:m:s)	−80:28:08.8	<i>Gaia</i> DR2
Epoch	2015.5	<i>Gaia</i> DR2
Parallax (mas)	54.705 ± 0.067	<i>Gaia</i> DR2
μ_{ra} (mas yr ^{−1})	311.19 ± 0.13	<i>Gaia</i> DR2
μ_{dec} (mas yr ^{−1})	1048.85 ± 0.14	<i>Gaia</i> DR2
<i>Gaia</i> DR2 ID	4623036865373793408	
HD ID	HD 39091	
TIC ID	261136679	
TOI ID	144.01	
Spectroscopic properties		
T_{eff} (K)	6037 ± 45	Ghezzi et al. (2010)
$\log g$ (cgs)	4.42 ± 0.03	Ghezzi et al. (2010)
[Fe/H] (dex)	0.08 ± 0.03	Ghezzi et al. (2010)
$v \sin i$ (km s ^{−1}) . .	3.14 ± 0.50	Valenti & Fischer (2005b)
Photometric properties		
B (mag)	6.25	
V (mag)	5.67	
<i>TESS</i> (mag)	5.1	TIC V7
<i>Gaia</i> (mag)	5.491	<i>Gaia</i> DR2
<i>Gaia</i> _r (mag)	5.064	<i>Gaia</i> DR2
<i>Gaia</i> _b (mag)	5.838	<i>Gaia</i> DR2
J (mag)	4.87 ± 0.27	2MASS
H (mag)	4.42 ± 0.23	2MASS
K_s (mag)	4.241 ± 0.027	2MASS
Derived properties		
M_* (M_{\odot})	1.094 ± 0.039	this work
R_* (R_{\odot})	1.10 ± 0.023	this work
L_* (L_{\odot})	1.444 ± 0.02	this work
Age (Gyr)	$2.98^{+1.4}_{-1.3}$	this work
Distance (pc)	18.27 ± 0.02	<i>Gaia</i> DR2
ρ_* (g cm ^{−3})	1.148 ± 0.065	this work

An independent analysis of the *TESS* data has also been reported by Gandolfi et al. (2018). We acknowledge the use of TESS Alert data, which is currently in a beta test phase, from the TESS Science Office. Funding for the TESS mission is provided by NASA’s Science Mission directorate. This research has made use of the Exoplanet Follow-up Observation Program website, which is operated by the California Institute of Technology, under contract with the National Aeronautics and Space Administration under the Exoplanet Exploration Program. CXH, JB, and MNG acknowledge support from MIT’s Kavli Institute as Torres postdoctoral fellows. AV’s work was performed under contract with the California Institute of Technology / Jet Propulsion Laboratory funded by NASA through the Sagan Fellowship Program executed by the NASA Exoplanet Science Institute. JAD and JNW acknowledge support from the Heising–Simons Foundation. SU, FP, FB, DS, CL, DE, M.Marmier, and M.Mayor acknowledge financial support from the Swiss National Science Foundation (SNSF) in the frame work of the National Centre for Competence in Research Plan-

etS. DE acknowledges financial support from the European Research Council (ERC) under the European Unions Horizon 2020 research and innovation program (project FOUR ACES; grant agreement 724427). NN acknowledges partial supported by JSPS KAKENHI Grant Number JP18H01265 and JST PRESTO Grant Number JPMJPR1775. D.D. acknowledges support provided by NASA through Hubble Fellowship grant HSTHF2-51372.001-A awarded by the Space Telescope Science Institute, which is operated by the Association of Universities for Research in Astronomy, Inc., for NASA, under contract NAS5-26555. We made use of the Python programming language (Rossum 1995) and the open-source Python packages NUMPY (van der Walt et al. 2011), EMCEE (Foreman-Mackey et al. 2013b), and CELERITE (Foreman-Mackey et al. 2017).

We acknowledge the traditional owners of the land on which the AAT stands, the Gamilaraay people, and pay our respects to elders past and present.

Facilities: *TESS*, HARPS, AAT.

REFERENCES

- Bryan, M. L., Knutson, H. A., Fulton, B., et al. 2018, ArXiv e-prints, arXiv:1806.08799 4
- Butler, R. P., Wright, J. T., Marcy, G. W., et al. 2006, ApJ, 646, 505 2
- Cameron, A. C. 2012, Nature, 492, 48 2
- Claret, A. 2017, A&A, 600, A30 3
- Diego, F., Charalambous, A., Fish, A. C., & Walker, D. D. 1990, in Proc. SPIE, Vol. 1235, Instrumentation in Astronomy VII, ed. D. L. Crawford, 562–576 2
- Dotter, A., Chaboyer, B., Jevremović, D., et al. 2008, ApJS, 178, 89 3
- Ehrenreich, D., Bourrier, V., Wheatley, P. J., et al. 2015, Nature, 522, 459 4
- Foreman-Mackey, D., Agol, E., Ambikasaran, S., & Angus, R. 2017, The Astronomical Journal, 154, 220 10
- Foreman-Mackey, D., Hogg, D. W., Lang, D., & Goodman, J. 2013a, PASP, 125, 306 3
- . 2013b, PASP, 125, 306 10
- Gaia Collaboration, Brown, A. G. A., Vallenari, A., et al. 2018, A&A, 616, A1 2
- Gandolfi, D., Barragan, O., Livingston, J., et al. 2018, ArXiv e-prints, arXiv:1809.07573 10
- Ghezzi, L., Cunha, K., Smith, V. V., et al. 2010, ApJ, 720, 1290 3, 9
- Günther, M. N., Queloz, D., Gillen, E., et al. 2017, MNRAS, 472, 295 2
- Günther, M. N., Queloz, D., Gillen, E., et al. 2018, Monthly Notices of the Royal Astronomical Society, 478, 4720 3
- Hadden, S., & Lithwick, Y. 2017, AJ, 154, 5
- Jenkins, J. M., Caldwell, D. A., Chandrasekaran, H., et al. 2010, ApJ, 713, L87 2
- Jones, H. R. A., Paul Butler, R., Tinney, C. G., et al. 2002, MNRAS, 333, 871 2
- Kempton, E. M.-R., Bean, J. L., Louie, D. R., et al. 2018, PASP, 130, 114401 3
- Kreidberg, L. 2015, PASP, 127, 1161 3
- Lo Curto, G., Pepe, F., Avila, G., et al. 2015, The Messenger, 162, 9 2
- Lopez, E. D., Fortney, J. J., & Miller, N. 2012, ApJ, 761, 59 7
- Mandel, K., & Agol, E. 2002, ApJ, 580, L171 3
- Mayor, M., Pepe, F., Queloz, D., et al. 2003, The Messenger, 114, 20 2
- Owen, J. E., & Wu, Y. 2017, ApJ, 847, 29 3
- Ranalli, P., Hobbs, D., & Lindegren, L. 2018, A&A, 614, A30 4
- Ricker, G. R., Winn, J. N., Vanderspek, R., et al. 2015, Journal of Astronomical Telescopes, Instruments, and Systems, 1, 014003 2
- Rossum, G. 1995, Python Reference Manual, Tech. rep., Amsterdam, The Netherlands, The Netherlands 10
- Seager, S., Kuchner, M., Hier-Majumder, C. A., & Militzer, B. 2007, ApJ, 669, 1279 7
- Seager, S., & Mallén-Ornelas, G. 2003, ApJ, 585, 1038 3
- Spake, J. J., Sing, D. K., Evans, T. M., et al. 2018, Nature, 557, 68 4
- Triaud, A. H. M. J. 2017, The Rossiter-McLaughlin Effect in Exoplanet Research, 2 4
- Vanderburg, A., Becker, J. C., Buchhave, L. A., et al. 2017, AJ, 154, 237 3
- Valenti, J. A., & Fischer, D. A. 2005a, ApJS, 159, 141 4
- . 2005b, ApJS, 159, 141 9
- van der Walt, S., Colbert, S. C., & Varoquaux, G. 2011, Computing in Science & Engineering, 13, 22 10
- Van Eylen, V., & Albrecht, S. 2015, ApJ, 808, 126
- Winn, J. N. 2010, Exoplanet Transits and Occultations, ed. S. Seager (University of Arizona Press), 55–77 3
- Winn, J. N., & Fabrycky, D. C. 2015, ARA&A, 53, 409 4
- Wittenmyer, R. A., Horner, J., Tuomi, M., et al. 2012, ApJ, 753, 169 2
- Zeng, L., Sasselov, D. D., & Jacobsen, S. B. 2016, ApJ, 819, 127 7
- Zhu, W., & Wu, Y. 2018, AJ, 156, 92 4
- Zurlo, A., Mesa, D., Desidera, S., et al. 2018, MNRAS, 480, 35 2, 4

TABLE 2
PARAMETERS FOR THE HD 39091 PLANETARY SYSTEM.

Additional RV parameters	RV offset	Instrument jitter
AAT (m s^{-1})	32.07 ± 0.86	6.7 ± 0.60
HARPS pre-fix (m s^{-1}) ...	108.51 ± 0.40	2.33 ± 0.18
HARPS post-fix (m s^{-1}) ..	130.60 ± 0.70	1.74 ± 0.33
Planet Parameters	Planet b	Planet c
P (days)	2093.07 ± 1.73	6.2679 ± 0.00046
T_p (BJD)	2445852.0 ± 3.0	-
T_c (BJD)	2446087.0 ± 8.4	$2458325.50400^{+0.0012}_{-0.00074}$
K (m s^{-1})	192.6 ± 1.4	$1.58^{+0.26}_{-0.28}$
$\sqrt{e} \cos \omega$	0.6957 ± 0.0044	-
$\sqrt{e} \sin \omega$	-0.392 ± 0.006	-
e	0.637 ± 0.002	0
ω	330.61 ± 0.3	-
T_{14} (hrs)	-	2.953 ± 0.047
a/R_\star	-	13.38 ± 0.26
R_p/R_\star	-	$0.01703^{+0.00025}_{-0.00023}$
$b \equiv a \cos i/R_\star$	-	$0.59^{+0.018}_{-0.020}$
i_c (deg)	-	$87.456^{+0.085}_{-0.076}$
Derived parameters		
M_p	$10.02 \pm 0.15 M_J$	$4.82^{+0.84}_{-0.86} M_\oplus$
R_p (R_\oplus)	-	2.042 ± 0.050
ρ_p (g cm^{-3})	-	$2.97^{+0.57}_{-0.55}$
$\log g_p$ (cgs)	-	$3.041^{+0.07}_{-0.86}$
a (AU)	3.10 ± 0.02	0.06839 ± 0.00050
T_{eq} (K) ^h	-	$1169.8^{+2.8}_{-4.3}$
$\langle F_j \rangle$ ($10^9 \text{ erg s}^{-1} \text{ cm}^{-2}$) ...	-	$0.42^{+0.04}_{-0.09}$